Simulation of Welding Deformation for Accurate Ship Assembly (Report III)

-Out-of-Plane Deformation of Butt Welded Plate-

Si Mei GU*, Hidekazu MURAKAWA**, Yukio UEDA,***
Yasuhisa OKUMOTO**** and Morinobu ISHIYAMA*****

Abstract

In this research, a 3-D thermal-elastic-plastic FEM is developed to simulate out-of-plane deformation caused by one-sided automatic submerged arc welding. Efforts have been made to improve the reliability and accuracy of the FEM calculation. To prevent the phenomenon of transverse-shear-locking, which is observed as overestimation of the stiffness of a plate for a bending problem when solid elements are used, a reduced integration method is employed and proved to be effective. A special type of spring-element is utilized to deal with the contact problem between the plate and the working table.

Using the 3-D FEM, the effects of various factors, such as gravity, the method of supporting, magnetic constraint and the force from the backing near the welding line have been investigated. The results from the numerical simulation can reasonably explain the phenomena observed from real situations in shipyards. In the case of FCB automatic submerged arc welding which has the features of large heat input, out-of-plane welding deformation is mainly affected by constraint conditions. The gravity of the plate and the backing force have great influence on the shape of angular distortion. Magnetic constraint can reduce the welding deformation effectively.

KEY WORDS: (Butt Welding) (Welding Deformation) (Out-of Plane Deformation) (FEM) (Contact Problem) (Magnetic Constraint) (Initial Deformation) (Gravity)

1. Introduction

In shipyards, great efforts have been made to speed up automation and mechanization in recent years in order to reduce the cost of building a ship and solve the problem of lacking skilled workers. It becomes one of the key problems to reduce the deformation resulting from flame cutting and welding because much higher precision is required in automation and mechanization. In addition to this, the errors occurring at the present assembly stage can have large influence on the precision of the next processes. Therefore, it is necessary to clarify various factors influencing precision, not only in particular assembly processes, but also between different processes. For the above reasons, the authors have conducted a series of researches based on thermal-elastic-plastic finite element methods to investigate the phenomena observed in shipyards under real working conditions. These include a study of the precision of flame cutting [1] and two reports [2),3] with emphasis on in-plane transverse shrinkage due to one-sided automatic submerged arc welding. The first report investigated the influences of welding and constraint conditions and the second examined the effects of correcting groove gaps caused by geometrical errors along cut edges. In this paper, out-of-plane deformation is discussed and the main attention is focused on angular distortion, which is one of the welding deformations often causing problems in assembly of ship structures.

2. Three Dimensional Numerical Simulation

2.1 Method of analysis

Although out-of-plane deformation caused by welding is a three dimensional problem, it was simplified to a two dimensional case by only considering angular distortion

† Received on May 21, 1996
* Graduate Student, Osaka University
** Associate Professor
*** Professor, Kinki University
**** Associate Professor, Kinki University
***** Ishikawajima-Harima Heavy Industries Co., Ltd.
Transactions of JWRI is published by Joining and Welding Research Institute of Osaka University, Ibaraki, Osaka 567, Japan.

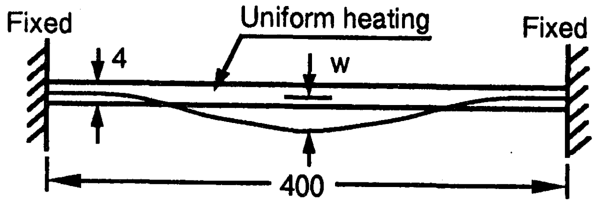

Fig.1 Buckling of beam under thermal expansion.

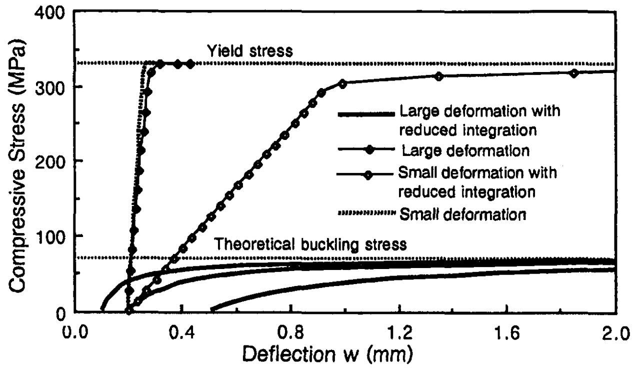

Fig.2 Comparison among different Finite Element Models.

in a central section perpendicular to the welding line[4),5)]. This kind of simplification ignores the influence of plate length and makes the results of simulation deviate from real situations as will be discussed in section 2.3. Furthermore, it is impossible to obtain important information on the deformation of end parts of the plate. The out-of-plane deformation at the ends of the plate is usually very complicated and larger in magnitude. The reason for the simplification is mainly that three dimensional analysis needs a huge amount of memory and computing time. It was almost impossible to perform three dimensional simulation on a large plate about two decades ago, although the thermal-elastic-plastic FEM theory for welding problem was established then[6)]. With the rapid development of computer technology, however, a so-called workstation, which in its performance is a mini-super-computer has been in commonly use. It makes 3-D numerical simulation of welding deformation acceptable both in economics and computing time.

To identify the important factors for out-of-plane welding deformation, a 3-D thermal-elastic-plastic FEM with considering large deformations is developed. A reduced integration method is employed to prevent transverse-shear-locking which is observed as overestimation of the stiffness of a plate for a bending problem when solid elements are used. A special type of spring-element is introduced to deal with the contact of steel plates with a working table under the gravity. The accuracy and feasibility of the program are verified by thermal buckling of a column and through a comparison between calculations and experiments on angular distortion due to the welding. Using the 3-D FEM, effects of various factors, such as gravity, the method of support, the distribution of heat input, the force from the backing and the magnetic constraint, are investigated.

A new 3-D FEM program named JWRIAN-W94 is specially developed for welding deformation. The theory of thermal-elastic-plastic FEM proposed by Ueda and Yamakawa[6)] is basically adopted and large deformation is also considered to deal with the geometrical non-linear problems such as buckling. An 8-node isoparametric solid element is used. Two improvements are made to improve the accuracy and to account for the real boundary condition in 3-D computation. One is for the transverse-shear-locking that is observed when solid elements are used. Another is for the contact between plates and the working table resulting from gravity. As the steel plates used in shipyards are very large, the contact condition is very complicated and can greatly affect the out-of-plane deformation. As in 2-D finite element simulations, transient temperature fields are obtained through solving heat conduction equations. Stress and deformation are calculated based on the computed temperature fields through thermal-elastic-plastic analysis. Temperature dependency of thermal and mechanical properties is considered in the same manner as the previous reports[2),3)]. In these reports, dummy elements were used to simulate the deposition of weld metal for 2-D welding problems. Whereas in this research, a method closer to the real situation is employed to lead to a better convergence rate in iterations. Those elements which represent weld metal do not exist at all before the electrodes reach their positions and are introduced after the electrodes pass their locations. All the following computations are carried out on the workstation YHP 9000-735.

2.2 Transverse shear locking and its prevention

It is known that when solid elements are used for the bending problem of thin plates, the computed deflection is less than the actual one. This overestimation of bending stiffness is called transverse-shear-locking. It is caused by the transverse shear stiffness which holds the plate from bending. To prevent this, a reduced integration method is effectively introduced. The method is based on the assumption that out-of-plane transverse shear strains and non-linear strains are constant within the element. Thus, the center of an element is chosen as the integration point for these terms. Gaussian points are 2*2*2 for linear terms of normal strains and in-plane transverse shear strains. The transverse shear strains and non-linear terms of all components of strains are

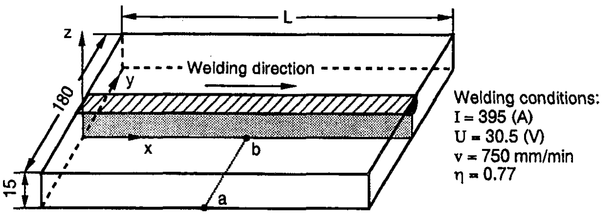

Fig. 3 Model and welding conditions for bead-on-plate welding.

integrated using one Gaussian point in the center of elements.

The effectiveness of the reduced integration method is verified by a buckling problem illustrated in **Fig.1**. An initially deformed column with build-in ends is uniformly heated. The column is 400 mm in length, 5 mm in width and 4 mm in thickness. Modules of elasticity and yield stress are assumed to be 210,000 MPa and 330 MPa, respectively. Three kinds of initial deflections of 0.1, 0.2 and 0.5 mm at the middle of the column are considered in FEM simulations. Assuming that the temperature is increased from 0 °C to about 190 °C, the change of deflection is computed using the four different finite element models. Two are based on the theory of small deformations with and without using the reduced integration method. The other two are large deformations with and without the reduced integration method. In FEM simulation, half of the column is taken and divided into 20 solid elements. **Figure 2** shows the computed results. The abscissa indicates the deflection at the middle of the column and the ordinate shows axial compressive stress. With the increase of temperature, thermal expansion causes compressive stress and makes the column buckle. According to Euler's formula, elastic buckling stress is about 69 MPa which is much smaller than the yield stress. Therefore, the compressive stress will not exceed the buckling stress if the result is reasonable. Comparison among the four models with the same initial deflection of 0.2 mm is made. Because non-linear terms are neglected, the compressive stress exceeds the buckling stress and almost reaches the yield stress in the cases of small deformations. It can be seen that although the use of the reduced integration method improves the bending stiffness and increases the deflection, no buckling occurs. In the case of large deformations and without the reduced integration method, significant reduction of the bending stiffness is not observed. Only in the case that both the large deformation theory and the reduced integration method are used, dose the compressive stress agree well with the Euler buckling stress. The same behavior is obtained for different initial deflections of 0.1 mm and 0.5 mm. The deflection increases rapidly when the compressive stress becomes close to the buckling stress. This means that only a finite element model that uses large deformation theory and a reduced integration method can provide an acceptable numerical result.

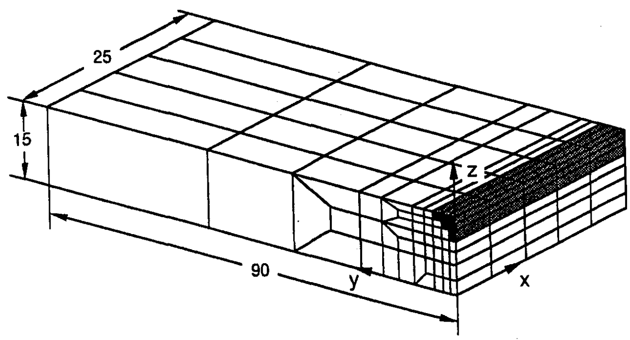

Fig. 4 Mesh division for simulation of bead-on -plate welding.

In butt welding, the bending stiffness of the plate is usually quite small as the thickness of the plate is much less than its length or width. A significant effect of in-plane stress, produced by thermal expansion and contraction in welding, on the out-of-plane deformation of the plate is expected. Thus, it is necessary to employ large deformation theory to simulate this type of deformation. On the other hand, temperature distribution is not uniform in the width, length and thickness directions. To represent such three dimensional phenomena, solid elements should be employed. For the above reasons, the finite element model considering large deformation and employing the reduced integration method is chosen for all the following numerical simulations of out-of-plane deformation.

2.3 Simulation of angular distortion of strips under welding

As a preparation for the numerical simulation of welding deformation of real size plates, the accuracy of the FEM is investigated through a comparison between the computed results and the experimental measurements by Tsuji[4]. The experiments were carried out on strips with different lengths and fixed width of 180 mm and thickness of 15 mm, as shown in **Fig. 3**. Angular distortions were measured and discussion was made based on a 2-D finite element analysis.

In this study, to simulate the experiments by 3-D FEM, one half of the specimen divided by the welding line which is the axis of symmetry is subdivided into the FEM mesh. **Figure 4** shows an example of a specimen with the length L being 25 mm. The plate near the welding line is divided into 7 layers to account for the temperature distribution in the thickness direction. Only

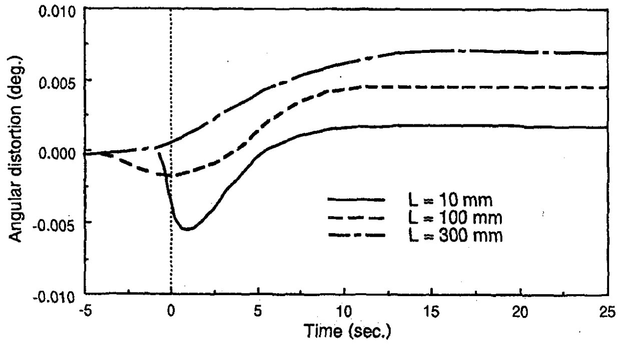

Fig.5 Transient angular distortion during welding.

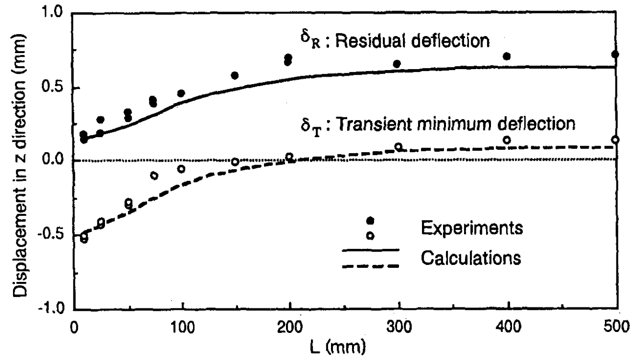

Fig.6 Comparison between experimental and computed angular distortions.

one layer is used for the area away from the welding line, where both temperature and its gradient are small. In experiments, a V-shape groove with the depth of 3.5 mm is formed in the middle of the plates. One-pass bead-on-plate welding is then laid along the groove. In simulation, the hatched elements are treated as weld metal using the technique described in section 2.1. Net heat input of welding is added into these elements for the computation of temperature field. Using the computed temperature, deformation is obtained by thermal-elastic-plastic computation. **Figures 5** and **6** show the results. Figure 5 is the transient angular distortion in the middle transverse section a-b for plates with their lengths of 10, 100 and 300 mm. The zero shown on the abscissa corresponds to the time when the welding arc reaches the middle transverse section. When the length is short and equal to 10 mm, the expansion of the heated area makes the strip deform downward in the heating stage. The downward angular distortion decreases with the cooling of the heated area and a reversed deformation occurs. The residual angular distortion is upward. It can be seen that as the plate is short, the temperature along the length is quite uniform. Thus the plate deforms quite freely with thermal expansion and contraction. When the plate is long, transient deformation is prevented by the stiffness of the plate before the arc and the contraction of the bead behind it. The transient downward deformation decreases and residual upward deformation increases with the increase of plate length. The effect of length on angular distortion is quantitatively shown in Fig. 6. δ_T is the minimum deflection which the point a (in Fig.3) ever experiences after the arc passes the middle transverse section. δ_R shows residual deflection at point a. Both δ_T and δ_R give relative deflections between points a and b. Open and solid circles represent experimental results and thick and broken lines indicate the computed results. The computed results agree well with experiments in both magnitude and tendency. It can be observed that transient deflection decreases by about the same amount as the residual deflection increases with the increase of the plate length. When the plate length is longer than 200 mm, the changes in δ_T and δ_R become very small and they approach constant values.

The agreement between the computation and the experiment suggests that the newly developed 3-D FEM program is a very effective method for the analysis of out-of-plane deformation caused by welding.

3. Modeling of Gravity and Contact between Plate and Working Table

It is known that welding conditions, size and shape of plate have a great influences on welding deformation. In addition to these factors, constraint condition is also considered to be a very important factor. In the case of FCB automatic submerged arc welding, which has the feature of a large heat input, the area with a temperature higher than the mechanical melting point is extremely long in the welding direction and wide in width. As the rigidity of this part is nearly zero, there is little resistance to transient deformation until the temperature near the welding line decreases below the mechanical melting point. Therefore, constraint conditions will have a great influence on welding deformation. On the other hand, the skin plates used for ship structures are commonly about 3 m in width and longer than 10 m. For the welding at large heat inputs on such big plates, the gravity acting on plates should be considered. At the same time, the constraint methods used in shipyards and the contact condition between plates and working table should also be taken into consideration to make the simulation reliable.

3.1 FEM modeling of gravity

The gravity is converted to the equivalent nodal force using the following equation which is standard in FEM[7] theory ;

$$\{f\}_z = \int_V [N]^T \varrho\, g\, dV$$

where $\{f\}_z$: equivalent nodal force corresponding to gravity

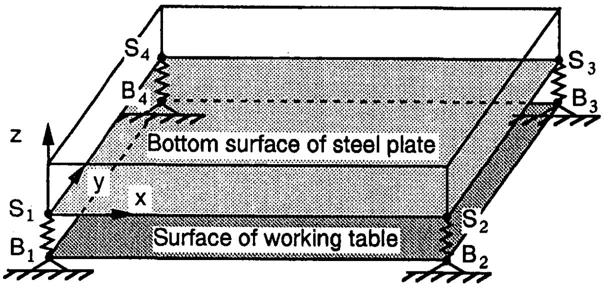

Fig.7 Special element for contact problem.

Table 1 Relations of spring constant K, nodal displacement Ws and spring force F.

State of spring	Contact	No Contact
Spring constant	$K \neq 0$	$K = 0$
Elongation	$W_s < 0$	$W_s \geq 0$
Spring force	$F < 0$	$F = 0$

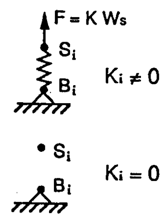

$[N]$: interpolation function matrix
ρ : density
g : gravitational acceleration
V : volume of an element

3.2 FEM modeling of contact problem

The gravity of a plate is balanced by reaction forces from the working table. Usually, plates keep contact with working table only in some places because of the shape of working table and the deformation of the plate. The plate is distorted during and after welding by thermal expansion and contraction. The condition of contact between plates and working table is very complicated because contact positions change with time and are also affected by the method of external constraint, such as backing under the welding line and magnetic constraint. To simulate various contact situations in the whole welding process, a spring element is introduced in FEM analysis.

As a relatively simple approach for solving the contact problem in numerical simulation, contact elements are introduced between the plate and the working table. Every contact element consists of four independent non-linear springs and each of the spring connects the nodes on the bottom surface of the plate and the top surface of the working table as shown in **Fig.7**. The relations among the spring constant K, the nodal displacement W_s and the reaction force F are shown in **Table 1**. Such non-linear spring element can be generated from the ordinary 8-node solid element in a simple manner as described in the following.

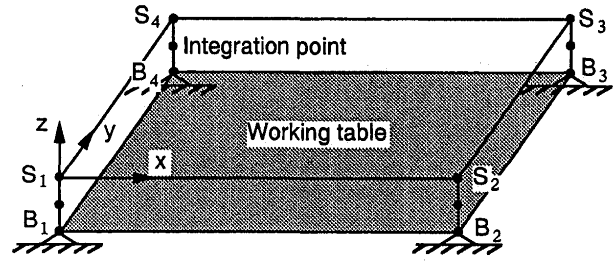

Fig.8 Forming of spring-element.

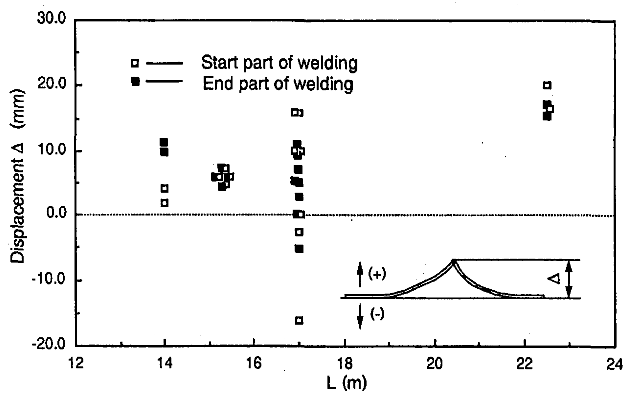

Fig.9 Measured displacements in z direction at both ends of plate welded by FCB welding.

1) moving integration points from normal positions to the center of four edges of the element S_1-B_1, S_2-B_2, S_3-B_3 and S_4-B_4 as shown in **Fig.8**;
2) of all components of the stress, only the normal component σ_z is considered and the strain energy $1/2E\ (\varepsilon_z)^2$ is used to evaluate the stiffness of the element;
3) the modulus of elasticity E is set as follows,

   when $\varepsilon_z < 0, E \neq 0$ (in contact)

   $\varepsilon_z \geq 0, E = 0$ (not in contact)

The judgment is carried out for every spring between the plate and the working table.

4. Out-of-Plane Deformation by FCB Automatic Submerged Arc Welding

4.1 Models to be analyzed

Experiments have been made to measure out-of-plane deformation of plates welded by FCB welding. The results are shown in Fig. 9. These show the measured displacements in the z direction at both ends of plates with different lengths. The tendency that the deflection increases with the length of the plate is observed. However, large variations in magnitude can also be observed. Concerning the direction of the deflection, it is upward in the majority of the cases but a few cases show downward deformation. From this experiment, it can be seen that the out-of-plane deformation of FCB welding

Table 2 List of cases for numerical simulation of FCB welding.

Computed cases	Plate size L×W×T (mm×mm×mm)	Gravity	Vertical support	Backing air force	Magnetic constraint	Initial deformation	Heating type
C1	3500×3000×16	Neglected	None	None	None	None	I
C2	3500×3000×16	Considered	Fully	None	None	None	I
C3	3500×3000×16	Considered	Partly	None	None	None	I
C4	3500×3000×16	Considered	Partly	None	None	None	II
C5	3500×3000×16	Considered	Fully	Considered	None	None	II
C6	3500×3000×16	Considered	Partly	Considered	Considered	None	II
C7	3500×3000×16	Considered	Partly	None	None	Considered	I

Table 3 FCB welding conditions.

Electrodes	Current (Amp.)	Voltage (Volt)	Speed (mm/min)	Groove shape
L	1180	33	680	50°
T_1	1130	37	680	50°
T_2	830	39	680	50°

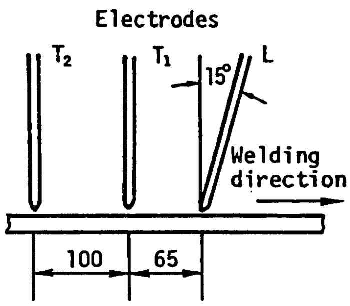

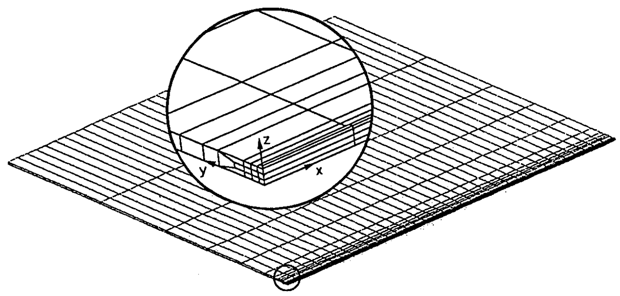

Fig.10 Mesh division for simulation of FCB welding.

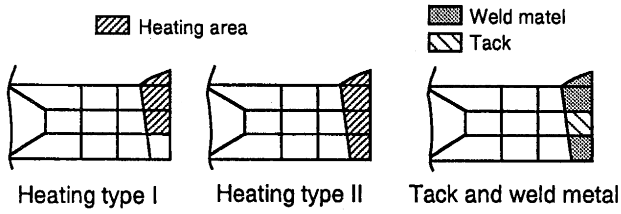

Fig.11 Types of heat input distribution and positions of tack welds.

involves uncertainty in its shape and large variation in its magnitude. As possible reasons for this, the variation in welding conditions, constraint conditions and initial imperfections are suspected. Thus, 7 cases listed in Table 2 are used to investigate various factors using 3-D thermal-elastic-plastic FEM considering gravity and the contact with working table. The size of the plate for simulation is 3.5 m in length, 3.5 m in width and 16 mm in thickness. As shown in Table 2, C1 is the case without considering gravity; C2 and C3 are cases considering both gravity and contact. In C2, the working table is assumed to have a plane surface to support the plates. It is also assumed that there is a long narrow gap with a width of 120 mm just below the welding line. No support is given to the plate in the open area of the gap. Whereas in C3, the gap is assumed to be very wide and the open space is 850 mm from the welding line. C4 differs from C3 in heating area to clarify the influence of the distribution of heat input. C5 and C6 are used to investigate the air force from the backing and the magnetic constraint. The effectiveness of magnets in reducing welding deformation is examined by C6. The effect of the initial deflection is studied using C7.

Considering geometrical symmetry, one of the two plates to be welded together is considered in FEM computations. **Figure 10** shows the mesh division with 3 layers near the welding line and 1 layer away from it. The coordinates x and y are chosen in the welding direction and in the transverse direction, respectively. The thickness direction is taken as z coordinate. The origin is so set that the x-y plane coincides with the bottom surface of the plate. The shape of the groove is like a capital letter Y with a 3 mm root as shown in **Table 3**. In the same table, welding conditions are also shown. Three sequential electrodes are used in the welding. In the simulation of the temperature field, the heat input is determined based on the contributions from the three electrodes. The efficiency of heat input is assumed to be 85%. The heat input per unit volume is calculated according to the welding speed and given uniformly into the heating area occupied by the three electrodes.

As shown in **Fig. 11**, two types of heat input distribution in transverse section perpendicular to the welding line are assumed. In type-I, the heat input is concentrated on the top side of the plate. Whereas in type-II, the heat input distributes relatively evenly in the thickness direction. In stress and strain computation, tack welding is approximated to be continuous along the welding line. Its position is located on the second layer from the bottom element, as shown in Fig. 11. Those elements representing welding metal exist only after the center of the electrodes reaches their positions.

4.2 Influences of gravity and constraint in z direction

Figure 12 shows computed out-of-plane deformation of C1 in which gravity is not considered. Angular distortions in three transverse sections, locating at the start, middle and end of the plate, are shown in Fig. 12(a). Figure 12(b) shows the displacements in the z direction along four longitudinal lines, which are from the line very close to the seam to the outer edge of the plate. It can be seen that the displacement along the welding line shows nearly symmetrical distribution with respect to the center of the plate. The deflection at the center of the plate near to the seam (y=17 mm) is about 10 mm. The deformation of the plate along the seam is convex. It can be seen that the angular distortion occurs only in the area very close to the seam and the plate away from the seam keeps an almost flat plane. On the other hand, angular distortion along the welding line is quite uniform. Significant difference is not observed between the middle part and the end parts. The doted line in Fig. 12(a) shows the angular distortion after exerting gravity on the deformed plate welded without gravitational force as a comparison. The deformation of the plate is obtained through elastic-plastic FEM simulation in which contact with the working table is taken into account. In this case, welding under gravity is divided into two independent processes, namely, the welding and the application of gravity. The maximum deflection computed in this way is about 6.5 mm. The plate near the welding line is deformed into a concave shape and the outer edge stays in touch with the working table because of the gravity.

Cases C2 and C3 are the numerical simulations of weldings under gravity. In C2, plates are welded on the working table which has the gap of 120 mm (D=60 mm) just below the welding line. In case of C3, this gap becomes a large opening with D=800 mm. The computed results of C2 are shown in **Fig. 13** in the same way as for C1 which shows the angular distortions in the three transverse sections and bending deformations along the four longitudinal lines. Compared with the dotted line in Fig. 12(a), the result from the separated processes of welding and application of gravity, maximum deflection decreases to 1/4, which is a small value of about 1.5 mm. The reason can be suggested that the transient welding deformation is restrained by gravity and it reduces the plastic strain produced near the welding line. Concerning the deflection along the welding line, its absolute value is small but the shape shows a concave form which is opposite to that in C1.

Figure 14 shows the results of C3 in which the gap is very wide. The dotted line in Fig.14(a) indicates the deformation in the central transverse section before welding. The deflection at the welding line due to gravity is as small as about 0.18 mm. After welding, the seam moves largely downwards and the deflection reaches about 10 mm. The plate deforms into the shape that only the outer edge of the plate (y=3000 mm) and the line corresponding to the inner edge of the working table (y=850 mm) are supported by the working table, leaving the plate between the two lines out of contact with the working table. The large opening in the working table lets the plate deform freely during welding, and causes a deflection much larger than C2. This situation is quite similar to C1 without gravity. In **Fig.15**, transient and residual deformations of C3 are shown. It is observed that large downward deflection occurs near the welding line where no support is given from the working table.

As the angular distortion caused by butt welding is largely affected by the temperature distribution in the thickness direction, comparison is made between heat inputs of type-I and type-II defined in section 4.1. As shown in Fig. 11, type-II gives relatively uniform heat input compared with the type-I. Type-I is applied in C3 and type-II in C4. The residual out-of-plane deformation for C4 is shown in **Fig.16**. The distribution of deflection is quite same as the deformation in C3, but the magnitude decreases by about 50 %. Although it is necessary to find out exact heating conditions under real

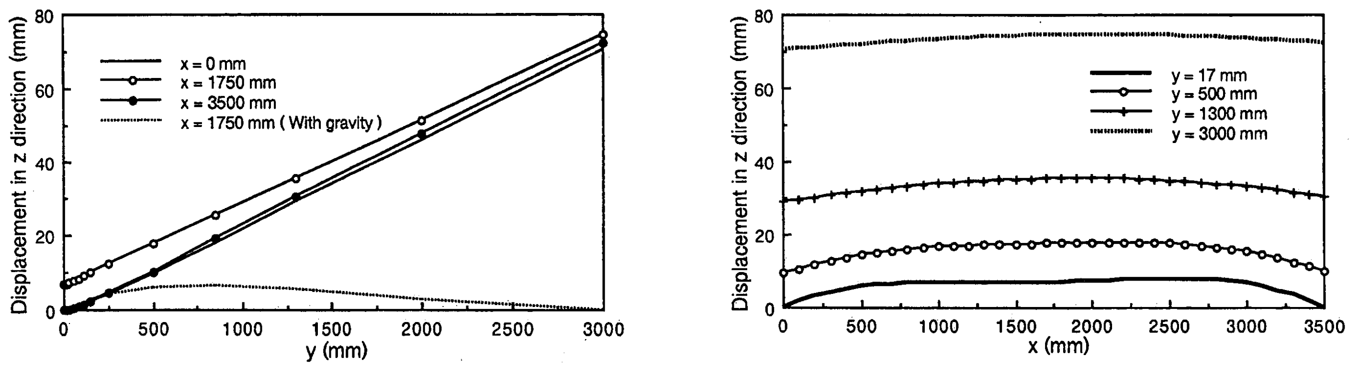

(a) Transverse section (b) Longitudinal section

Fig.12 Computed out-of-plane deformation (case C1).

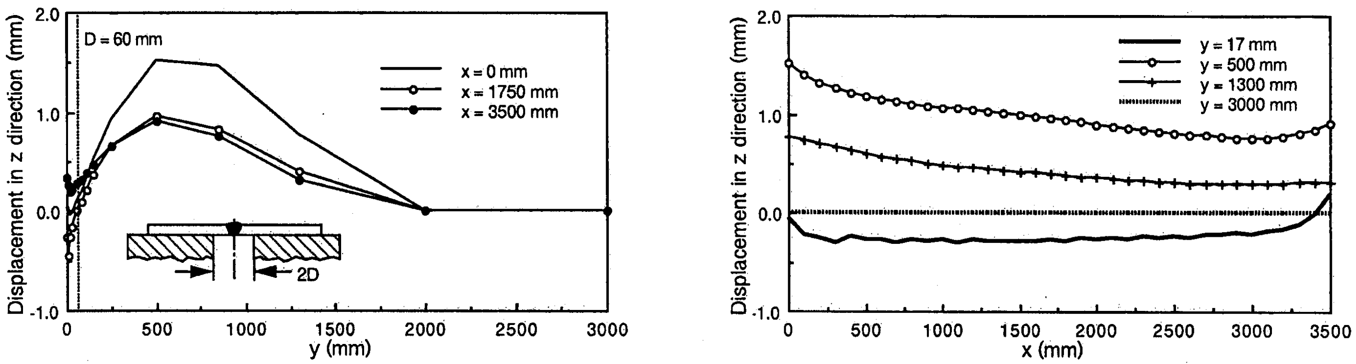

(a) Transverse section (b) Longitudinal section

Fig.13 Computed out-of-plane deformation (case C2).

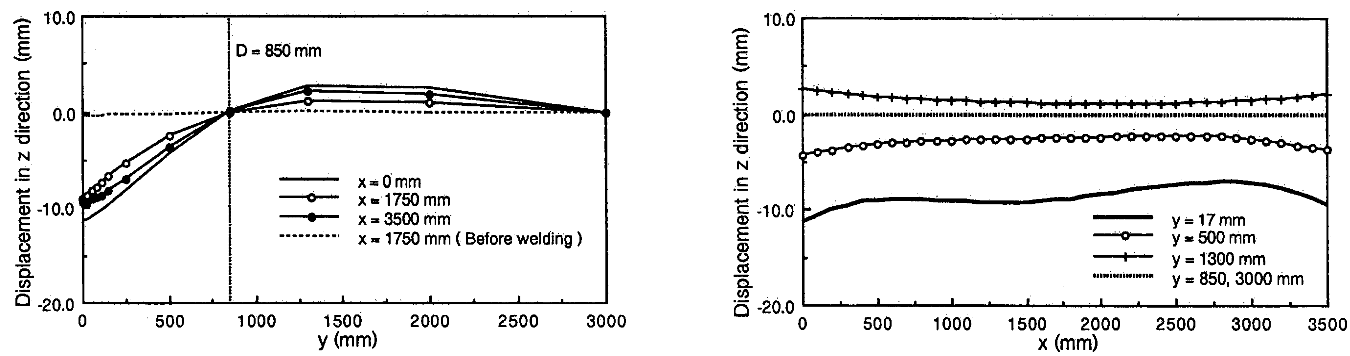

(a) Transverse section (b) Longitudinal section

Fig.14 Computed out-of-plane deformation (case C3).

welding to make the numerical simulation quantitatively reliable, two idealized heating types are used here for discussion because of the lack of available measured data.

4.3 Influences of backing force and magnetic constraint

In FCB one-sided automatic submerged arc welding, backings made of copper are set under the groove in order to get sound weld beads. To keep the backing in contact with the plate, the pressure from compressed air is used to hold the backing during the welding. Because of this air force, the plate near the welding line rises slightly. Since it may be an important factor influencing the out-of-plane deformation, the air force is introduced in the simulation of C5. The upward air force is assumed to be 130 kgf/m and is uniformly applied on the bottom surface near the welding line as a distributed external force, as shown in **Fig. 17**.

Figure 18 gives the residual deformation for this case. The dotted line in Fig.18(a) shows the deformation at the central transverse section before welding. The part of the plate 1300 mm away from the welding line is lifted up by the backing. The deflection is about 1.9 mm, 10 times larger than the deflection caused by gravity shown in C3. The deformation after welding shows the same shape as the initial one, which is a convex angular distortion. From the temperature distribution point of view, the residual angular distortion should be concave. In this case, however, it is surmised that the upward force from the compressed air becomes a dominant factor and it makes the residual deformation take an upward shape. Among the three angular distortions shown in Fig. 18(a), the deflections at the starting end and at the middle section are quite similar. The biggest deflection appears at the end of plate, being about 20 mm.

Another point worth noticing is that the deflection in C5 is very large. The reason is that the copper backing, pushed by the compressed air, lifts the plate near the welding line so that the plate can deform freely during the welding. This situation is quite like C3, in which the constraint from the working table is very small. To reduce the deflection, magnetic constraint is often utilized. Its effect is examined by simulating C6. Three magnets with 1.5 t attraction each are set along the plate of 3.5 m in length, as shown in Fig.17. In computation, the welding process considering both the backing force and the attraction of magnets is simulated first. Then, the residual deformation after cooling and removing both the air force and the magnets is computed. **Figure 19** shows the results. It is noted that the out-of-plane deformation differs from the cases discussed before. The angular

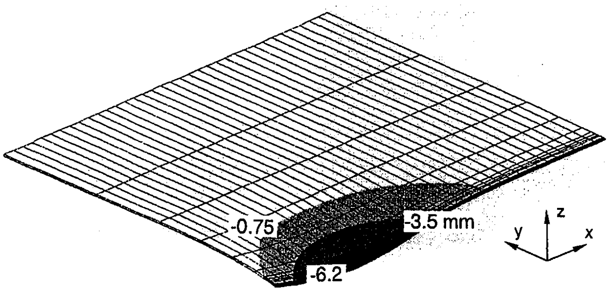

(a) Transient deformation

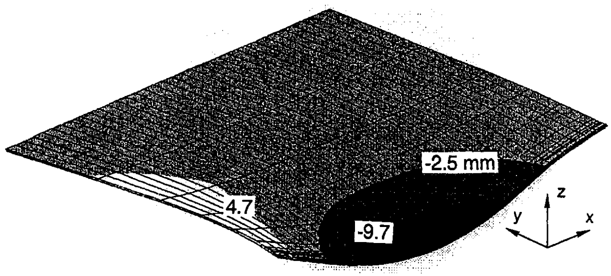

(b) Transient deformation

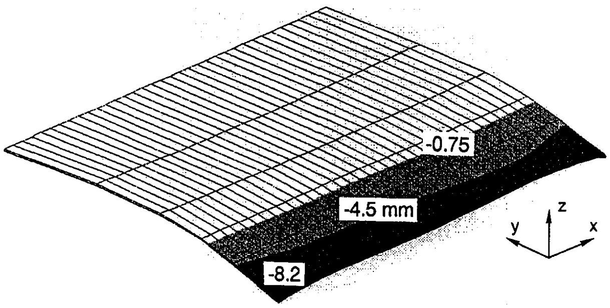

(c) Residual deformation

Fig.15 Welding deformation computed by 3-D FEM.

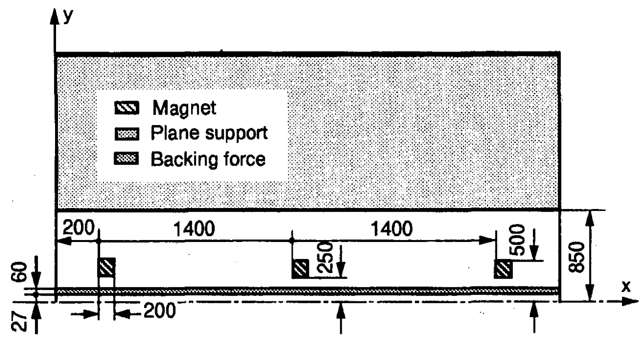

Fig.17 Arrangements of supports, magnet and backing force.

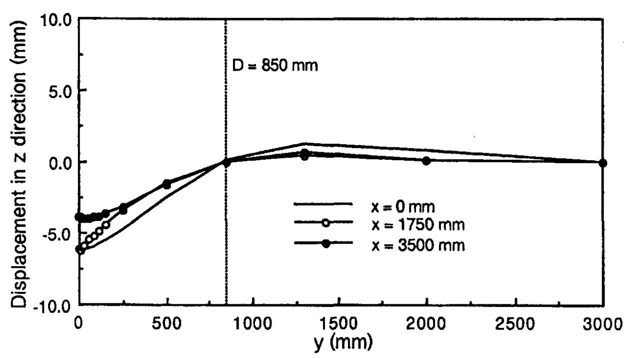

(a) Transverse section

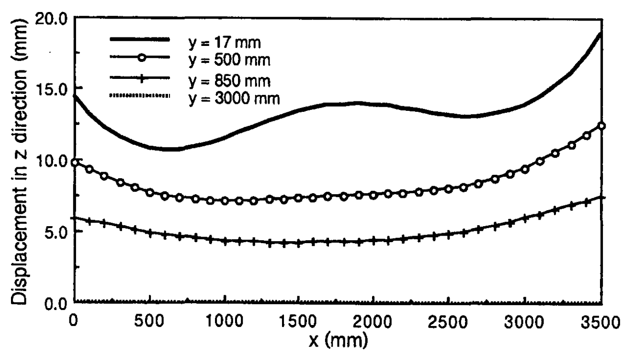

(b) Longitudinal section

Fig.16 Computed out-of-plane deformation (case C4).

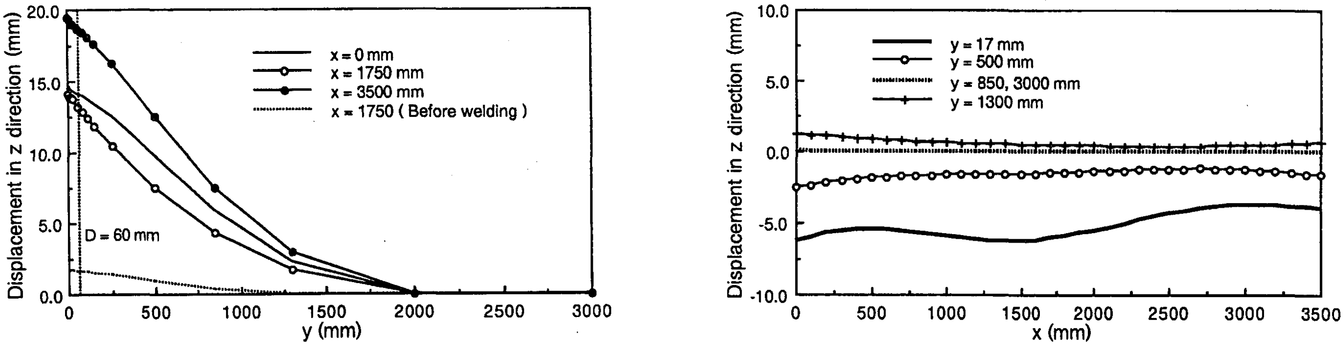

(a) Transverse section (b) Longitudinal section

Fig.18 Computed out-of-plane deformation (case C5).

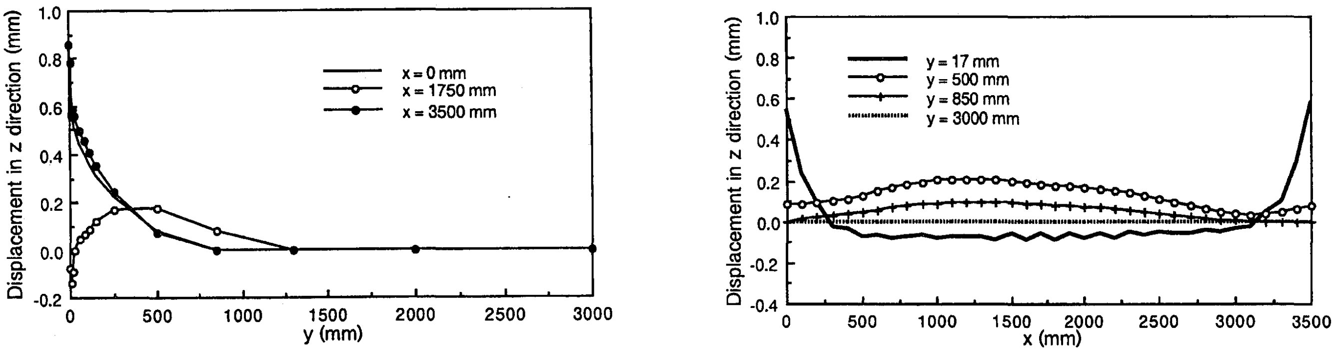

(a) Transverse section (b) Longitudinal section

Fig.19 Computed out-of-plane deformation (case C6).

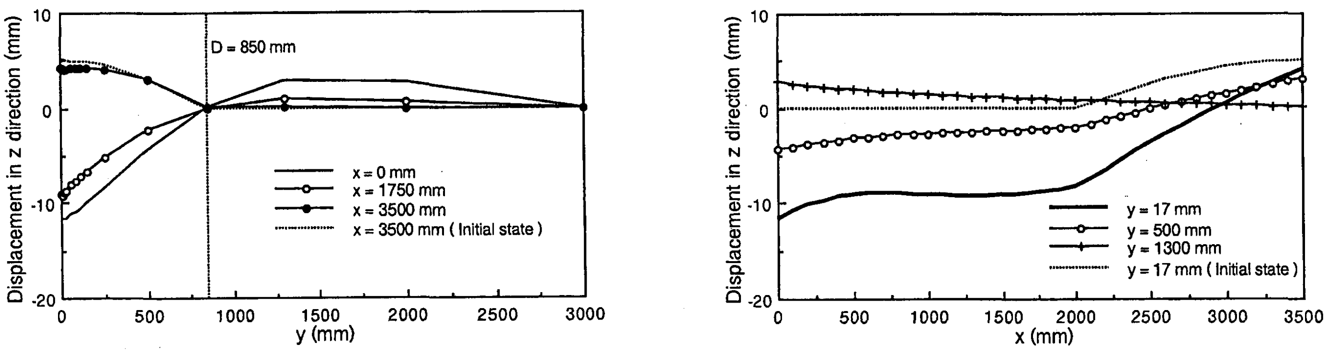

(a) Transverse section (b) Longitudinal section

Fig.20 Computed out-of-plane deformation (case C7).

distortions are convex at both ends and concave in the middle part. The maximum deflection is smaller than 1 mm, much less than the deflection of C5. The effectiveness of the magnetic constraint is confirmed through this simulation.

4.4 Influence of initial deformation

It is known from the measured data shown in Fig.9 that large variations exist in the shape of angular distortion and in its magnitude. In addition to the constraint condition, the deformation before the welding, which can be caused by tack and tab weldings may also be an influential factor. In C7, the initial deformation expressed by the following equation is considered.

$$z = z + 5\cos\left\{\frac{(3500-x)\pi}{3000}\right\}\cos\left(\frac{y\pi}{1700}\right) \quad (1)$$

where; x > 2000, |y| < 850 mm

The shape of the initial deflection is that the area 1.5 m from the end of the plate and 0.85 m from the welding line is deflected upward. The maximum deflection is 5 mm. The computed residual welding deformation for such initially deformed plates is shown in **Fig. 20**. It can be seen that both the shape and the magnitude of the deflection are almost the same as the deflection of C3 in the start and middle areas where no initial deformation exists. However, near the end of the plate, the residual deformation is greatly influenced by the initial deformation in the end part of the plate. The angular distortion turns to the convex shape when approaching the end of the plate.

5. Concluding Remarks

It is necessary to control and reduce the out-of-plane welding deformation for accurate ship assembly. FEM numerical simulation is an effective way to identify influential factors and to make quantitative predictions. In this research, a newly developed thermal-elastic-plastic FEM is used to simulate out-of-plane deformation produced by FCB butt welding. The main conclusions drawn are as follows:

1) As transverse-shear-locking is a problem affecting the accuracy of computation when solid elements are applied to a bending problem of thin plates, a selective reduced integration method is employed and proven to be very effective.
2) The accuracy and feasibility of the FEM program are verified through a good agreement between the measurements by Tsuji on angular distortion of steel strips and the numerical simulations.
3) As gravity has a large influence on the deformation in FCB butt welding, it is necessary to take account of the contact between plate and the working table.
4) To reduce welding deflection, densely arranged working tables or one with a flat surface is recommended. In other words, a working table with small spacing is better than a working table with large spacing.
5) The shape of angular distortion is affected by a number of factors, such as constraint conditions, backing force and initial deformation. Not all the angular distortions are concave with respect to the heating side. Some shows convex shape depending on the condition.
6) Forced constraint is an effective means of controlling angular distortion. For example, magnets can be used to balance the air force and to keep the steel plate in contact with the working table during welding.

Acknowledgment

The authors would like to acknowledge Mr. Tadao SAITOH (senior welding engineer, Ishikawajima-Harima Heavy Industries Co., Ltd) for his helpful comments and constructive discussions.

References

1) Y. Ueda, H. Murakawa, S. M. Gu, Y. Okumoto and M. Nakamura, "Simulation of Welding Deformation for Accurate Ship Assembling (2nd Report)", Transactions of JWRI, Vol. 22, No. 1(1993), pp. 135-144.
2) Y. Ueda, H. Murakawa, S. M. Gu, Y. Okumoto and M. Ishiyama, " FEM Simulation of Gas and Plasma Cutting with Emphasis on Precision of Cutting", Transactions of JWRI, Vol. 23, No. 1(1994), pp. 93-102.
3) Y. Ueda, H. Murakawa, S. M. Gu, Y. Okumoto and R. Kamichika, "Simulation of Welding Deformation for Accurate Ship Assembling (1st Report)", Transactions of JWRI, Vol. 21, No. 2(1992), pp. 265-275.
4) I. Tsuji and K. Ogawa, " An Analysis on Transient Stress and Deformation of a Steel Strip Subjected to Local Heating", Journal of the Japan Welding Society, Vol. 45, No. 1(1976), pp.36-41(in Japanese)
5) K. Satoh and T. Terasaki, "Effect of Welding Conditions on Welding Deformations in Welded Structural Materials", Journal of the Japan Welding Society, Vol. 45, No. 4(1976), pp.302-309 (in Japanese)
6) Y. Ueda and T. Yamakawa, "Analysis of Thermal Elastic-Plastic Behavior of Metals during Welding by Finite Element Method", Journal of the Japan Welding Society, Vol.42, No.6(1973),pp.567-577(in Japanese)
7) Yagawa and Miyazaki, " Analysis of Thermal Stresses, Creep and Thermal Conduction by Finite Element Method", Science Press(1985), pp.135-138(in Japanese)